CHEMISTRY
A EUROPEAN JOURNAL

DOI: 10.1002/chem.200701390

Divalent Carbon(0) Chemistry, Part 1: Parent Compounds

Ralf Tonner and Gernot Frenking*[a]

Abstract: Quantum-chemical calculations with DFT (BP86) and ab initio methods [MP2, SCS-MP2, CCSD(T)] have been carried out for the molecules $C(PH_3)_2$ (**1**), $C(PMe_3)_2$ (**2**), $C(PPh_3)_2$ (**3**), $C(PPh_3)(CO)$ (**4**), $C(CO)_2$ (**5**), $C(NHC_H)_2$ (**6**), $C(NHC_{Me})_2$ (**7**) $(Me_2N)_2C{=}C{=}C(NMe_2)_2$ (**8**), and NHC (**9**), where NHC = N-heterocyclic carbene and NHC_{Me} = *N*-methyl-substituted NHC. The electronic structure in **1**–**9** was analyzed with charge- and energy-partitioning methods. The results show that the bonding situations in L_2C compounds **1**–**8** can be interpreted in terms of donor–acceptor interactions between closed-shell ligands L and a carbon atom which has two lone-pair orbitals L→C←L. This holds particularly for the carbodiphosphoranes **1**–**3** where $L = PR_3$, which therefore are classified as divalent carbon(0) compounds. The NBO analysis suggests that the best Lewis structures for the carbodicarbenes **6** and **7** where L is a NHC ligand have C=C=C double bonds as in the tetraaminoallene **8**. However, the Lewis structures of **6**–**8**, in which two lone-pair orbitals at the central carbon atom are enforced, have only a slightly higher residual density. Visual inspection of the frontier orbitals of the latter species reveals their pronounced lone-pair character, which suggests that even the quasi-linear tetraaminoallene **8** is a "masked" divalent carbon(0) compound. This explains the very shallow bending potential of **8**. The same conclusion is drawn for phosphoranylketene **4** and for carbon suboxide (**5**), which according to the bonding analysis have hidden double-lone-pair character. The AIM analysis and the EDA calculations support the assignment of carbodiphosphoranes as divalent carbon(0) compounds, while NHC **9** is characterized as a divalent carbon(II) compound. The L→C(^{1}D) donor–acceptor bonds are roughly twice as strong as the respective L→BH_3 bond.

Keywords: bonding analysis · carbon complexes · carbon · density functional calculations · donor–acceptor systems

Introduction

Most organic compounds which are stable in a condensed phase have tetravalent carbon(IV) atoms, all four valence electrons of which are engaged in chemical bonds. A notable exception is the trivalent valence state of carbon in monocoordinate CO, which has been called "an isolated embarrassment for introductory chemistry teachers".[1,2] The rare trivalent valence state of carbon is also found in the recently synthesized[3] transition metal complexes that have a terminal carbon atom as ligand.[4] Molecules with divalent carbon atoms are usually identified with carbenes, where the carbon atom has one σ-type lone-pair orbital and a formal oxidation state of two. The divalent carbon(II) chemistry of carbene compounds received a major upswing in 1991 when Arduengo et al.[5] introduced imidazolin-2-ylidenes as synthetically useful stable molecules. Stable carbenes had already been isolated in 1985 by Bertrand et al.,[6] but phosphanylcarbenes were only later recognized as divalent C^{II} compounds.[7] The chemistry of carbenes has been greatly extended since the groundbreaking work of Arduengo et al. and Bertrand et al., and the scope of divalent carbon(II) chemistry has been significantly extended since the successful isolation of the first stable carbenes.[8]

Divalent carbon atoms may also have a formal oxidation state of zero rather than two. We recently reported a quantum-chemical analysis of the bonding situation in carbodiphosphoranes $C(PR_3)_2$ which showed that the C–PR_3 bonds should be discussed in terms of donor–acceptor interactions between the phosphorous lone-pair electrons and empty valence orbitals of carbon (Scheme 1).[9] Inspection of the

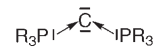

Scheme 1. Schematic representation of the bonding situation in carbodiphosphoranes.

[a] Dipl.-Chem. R. Tonner, Prof. Dr. G. Frenking
Fachbereich Chemie
Philipps-Universität Marburg
Hans-Meerwein-Strasse, 35032 Marburg (Germany)
E-mail: frenking@chemie.uni-marburg.de

Supporting information for this article is available on the WWW under http://www.chemeurj.org/ or from the author.

electronic structure revealed that the four valence electrons of carbon are not engaged in chemical bonding but are rather retained as two electron lone pairs. The bonding analysis indicated that carbodiphosphoranes (CDPs) have one σ-type lone-pair orbital and one π-type lone-pair orbital at the divalent C^0 atom. This is a unique bonding situation which conceptually distinguishes CDPs from carbenes.

Carbodiphosphoranes have been known experimentally since 1961, when Ramirez et al. synthesized $C(PPh_3)_2$ as a stable compound which melts at 208–210 °C.[10] They used several resonance forms to describe the carbon–phosphorus bonds in the molecule. Carbodiphosphoranes became the subject of intense experimental studies in the following years by several groups, and numerous compounds containing the CDP moiety could be isolated.[11] Interest in CDPs partly came from the finding that solid $C(PPh_3)_2$ exhibits the unusual property of light emission, which was dramatically observed as triboluminescence.[12]

The electronic structure in CDPs has sometimes been described in the past in terms of two electron pairs at carbon,[13] but the prevailing description of the bonding situation in carbodiphosphoranes either uses the notation $R_3P{=}C{=}PR_3$ or the bonding is compared with carbenes or ylides.[11] The delineation of the electronic structure with two lone pairs at carbon and with $C{\leftarrow}PR_3$ donor acceptor bonds explains the unusual chemical behavior of carbodiphosphoranes, which are very strong Lewis bases. For example, $C(PPh_3)_2$ readily reacts with CO_2 to give the adduct $(PPh_3)_2C{\rightarrow}CO_2$, which has a rather short donor–acceptor bond between the carbon atoms.[14] The availability of two carbon lone pairs in $C(PPh_3)_2$ comes to the fore in the isolation of the doubly protonated cation in the salt $[(PPh_3)_2CH_2][FeCl_4]_2$[15] and in the synthesis of the donor–acceptor complex $[(PPh_3)_2C(AuCl)_2]$.[16] The residual donor strength in singly protonated $(PPh_3)_2CH^+$ is still strong enough to permit the isolation of the triply charged complex $[\{(PPh_3)_2CH\}_2Ag]^{3+}$.[9] As a further probe of the four-electron donor strength of CDP we allude to the isolation of the stable complex $[(CO)_2Ni\{C(PPh_3)_2\}]$, in which $C(PPh_3)_2$ replaces two CO ligands.[17] Very recently, Petz et al. isolated and determined the X-ray structure of the first CDP complex with a bidentate main group Lewis acid bonded to the carbon atom, namely, $[\{(\mu\text{-}H)H_4B_2\}C(PPh_3)_2](B_2H_7)$, in which the carbon atom of $C(PPh_3)_2$ binds to both boron atoms of the cation $B_2H_5^+$.[18]

Carbodiphosphoranes may be considered as examples of molecules with general formula CL_2 in which the ligands L are Lewis bases which engage in a donor–acceptor bond with the carbon atom. We searched for other ligands L which might yield stable divalent carbon(0) compounds. Obvious choices are CO and N-heterocyclic carbenes (NHCs) because both are ubiquitous ligands in complexes. CO is usually considered to be a strong π-acceptor ligand,[19] but it can also bind as a σ donor without significant π-bonding contributions in nonclassical carbonyl complexes.[20] A comparative study of the nature of the bonding in the isoelectronic hexacarbonyls $[TM(CO)_6]^q$ ($TM^q = Hf^{2-}$, Ta^-, W, Re^+, Os^{2+}, Ir^{3+}) showed that the σ contribution exceeds π bonding in the positively charged complexes.[21] The ligand properties of NHCs are often compared to those of phosphines PR_3, because both ligands are thought to bind mainly through the σ lone pair.[22] A recent comparative investigation of $[TM(CO)_5L]$ for the Group 6 metals TM = Cr, Mo, W between L = NHC and $L = PMe_3$, PCl_3 showed that the NHC ligand is a stronger σ donor and a weaker π acceptor than phosphine ligands in these complexes.[23]

The CO homologues of $C(PR_3)_2$ are experimentally known. The mixed-ligand species $(R_3P)C(CO)$ with R = Ph has been isolated, and its geometry determined by X-ray structure analysis.[24] The P-C-C bending angle between the ligands of 145.5° is less acute than the P-C-P angle of 131.7° in $C(PPh_3)_2$. The former compounds were termed phosphaketene ylides whose bonding situation was described with double bonds $R_3P{=}C{=}C{=}O$.[11b] The dicarbonyl homologue $C(CO)_2$ is known as carbon suboxide C_3O_2, which was synthesized as early as 1906.[25] Experimental studies on C_3O_2 mainly focussed on the reactivity of the double bonds in the molecule, which is sketched as $O{=}C{=}C{=}C{=}O$.[26] Carbon suboxide has a quasi-linear equilibrium geometry with a remarkably shallow bending potential.[27] Divalent carbon(0) compounds with N-heterocyclic carbene ligands $C(NHC)_2$ are experimentally nearly unknown. The only experimental work which reports on the synthesis of carbodicarbenes that is known to us is a mass-spectrometric identification of a phenyl-annelated homologue of $C(NHC)_2$ by Grahn, which was described, however, as an allene derivative.[28] A singly C-protonated cation of an octamethyl derivative $[HC(NHC)_2]^+$ has been isolated and an X-ray structure analysis was reported by Kuhn et al.[29] Very recently we reported quantum-chemical calculations on the parent compound $C(NHC_H)_2$ and the *N*-methyl substituted derivative $C(NHC_{Me})$ which predict that carbodicarbenes are viable goals for synthesis.[30]

Here we report on a comprehensive theoretical investigation of divalent carbon(0) compounds CL_2 where $L = PR_3$, CO, NHC. We optimized the geometries and calculated the energies of the molecules $C(PH_3)_2$ (**1**), $C(PMe_3)_2$ (**2**), $C(PPh_3)_2$ (**3**), $C(PPh_3)(CO)$ (**4**), $C(CO)_2$ (**5**), $C(NHC_H)_2$ (**6**), and $C(NHC_{Me})_2$ (**7**) using gradient-corrected density functional theory (BP86) and ab initio methods at the MP2 and CCSD(T) levels of theory. To compare the theoretically predicted properties of dicarbenes **6** and **7** with related compounds, we also calculated tetrakis(dimethylamino)allene $(Me_2N)_2C{=}C{=}C(NMe_2)_2$ (**8**) and imidazolin-2-ylidene (**9**), the parent N-heterocyclic carbene (NHC). The calculated compounds are shown in Scheme 2. The electronic structure of the molecules was analyzed with charge- and energy-decomposition methods.

To investigate the donor properties of **1**–**9** we also calculated the protonation energies, and we theoretically investigated donor–acceptor complexes of the compounds with the Lewis acids BH_3, CO_2, $W(CO)_5$, $Ni(CO)_3$ and $Ni(CO)_2$. The latter results are presented and discussed in the following paper in this issue.[31]

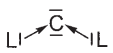

		No.
L =	PH_3	**1**
	PMe_3	**2**
	PPh_3	**3**
	PPh_3, CO	**4**
	CO	**5**
	NHC_H	**6**
	NHC_{Me}	7
	$C(NMe_2)_2$	**8**

9

Scheme 2. Molecules **1**–**9** which have been investigated in this work. NHC_H = N-heterocyclic carbene (imidazolin-2-ylidene). NHC_{Me} = *N*-methyl-substituted NHC.

Methods

Geometry optimizations without symmetry constraints were carried out with the Gaussian 03 optimizer[32] together with TurboMole5[33] energies and gradients at the BP86[34]/def-SVP[35] level of theory. For the phenyl rings of PPh_3 groups a minimal basis set was used (benzene BS) except for the α-C atom. Stationary points were characterized as minima by calculating the Hessian matrix analytically at this level of theory.[36] Thermodynamic corrections and Kohn–Sham orbitals were taken from these calculations. The standard state for all thermodynamic data is 298.15 K and 1 atm. Single-point energies at the BP86/def-SVP (in the following called SVP) optimized geometries were calculated with the MP2 method[37] with application of the frozen-core approximation for non-valence-shell electrons and with BP86 and the def2-TZVPP[38] basis set (in the following called TZVPP). The geometries of molecules **1**–**9** were also optimized with the program package ADF at the BP86/TZ2P level of theory, as outlined below. For the BP86 and the MP2 calculations the resolution-of-identity method was applied.[39] MP2 energies were also calculated with inclusion of the spin-component-scaled (SCS) correction proposed by Grimme[40] by applying the standard parameters. The NBO[41] analyses were carried out with the internal module of Gaussian 03 at the BP86/TZVPP level of theory. We also analyzed the electronic charge distribution with the Atoms-in-Molecules (AIM) method[42] which was performed at the BP86/TZVPP level of theory with a locally modified version of the AIMPAC program package.[43] CCSD(T)/TZVPP energies were calculated for some molecules with the program package Molpro2006.[44]

For bonding analysis some molecules were optimized with C_{2v} symmetry constraints with the program package ADF2006.01.[45] As above, BP86 was chosen with uncontracted Slater-type orbitals (STOs) as basis functions.[46] The latter basis sets for all elements have triple-ζ quality augmented by two sets of polarization functions (ADF basis set TZ2P). Core electrons (i.e., 1s for second- and [He]2s2p for third-row atoms including first-row transition metals, [Ne]3s3p3d for second-row and [Ar]4s4p4d for third-row transition metals) were treated by the frozen-core approximation. This level of theory is denoted BP86/TZ2P. An auxiliary set of s, p, d, f and g STOs was used to fit the molecular densities and to represent the Coulomb and exchange potentials accurately in each SCF cycle.[47] Scalar relativistic effects were incorporated by applying the zeroth-order regular approximation (ZORA) in all ADF calculations.[48]

The interatomic interactions were investigated by means of an energy-decomposition analysis (EDA) developed independently by Morokuma[49] and by Ziegler and Rauk.[50] The bonding analysis focuses on the instantaneous interaction energy ΔE_{int} of a bond A–B between two fragments A and B in the particular electronic reference state and in the frozen geometry of AB. This interaction energy is divided into three main components [Eq. (1)].

$$\Delta E_{int} = \Delta E_{elstat} + \Delta E_{Pauli} + \Delta E_{orb} \quad (1)$$

The term ΔE_{elstat} corresponds to the quasi-classical electrostatic interaction between the unperturbed charge distributions of the prepared atoms and is usually attractive. The Pauli repulsion ΔE_{Pauli} is the energy change associated with the transformation from the superposition of the unperturbed electron densities $\rho_A + \rho_B$ of the isolated fragments to the wavefunction $\Psi^0 = N\hat{A}[\Psi^A\Psi^B]$, which properly obeys the Pauli principle through explicit antisymmetrization ($\hat{A}$ operator) and renormalization (N = constant) of the product wavefunction.[45a] ΔE_{Pauli} comprises the destabilizing interactions between electrons of the same spin on either fragment. The orbital interaction ΔE_{orb} accounts for charge transfer and polarization effects.[51] The ΔE_{orb} term can be decomposed into contributions from each irreducible representation of the point group of the interacting system. Since the molecules in our study have at least C_s symmetry, it is possible to estimate the intrinsic strength of orbital interactions from orbitals having a′ (σ) and a″ (π) symmetry quantitatively. This directly gives the contributions of the σ and π orbital interactions to the ΔE_{orb} term [Eq. (2)]

$$\Delta E_{orb}(C_s) = \Delta E_{\sigma}(a') + \Delta E_{\pi}(a'') \quad (2)$$

Some molecules have C_{2v} symmetry, which makes it possible to distinguish between π contributions arising from in-plane (b_2) $\pi_{\parallel}$ orbitals and out-of-plane (b_1) $\pi_{\perp}$ orbitals [Eq. (3)]. The energy contributions from orbitals which have δ symmetry (a_2) are negligible for the investigated molecules.

$$\Delta E_{orb}(C_{2v}) = \Delta E_{\sigma}(a_1) + \Delta E_{\delta}(a_2) + \Delta E_{\pi\perp}(b_1) + \Delta E_{\pi\parallel}(b_2) \quad (3)$$

To obtain the bond dissociation energy (BDE) D_e (by definition with opposite sign to ΔE), the preparation energy ΔE_{prep}, which gives the relaxation of the fragments into their electronic and geometrical ground states, must be added to ΔE_{int} [Eq. (4)].

$$\Delta E(= -D_e) = \Delta E_{int} + \Delta E_{prep} \quad (4)$$

Further details on the EDA method[45] and its application to the analysis of the chemical bond[52] can be found in the literature.

Cartesian coordinates [Å] and total energies of all compounds discussed in the text are available as Supporting Information.

Results and Discussion

Geometries and energies: The optimized geometries of compounds **1**–**9** at the BP86/TZ2P and BP86/SVP levels are shown in Figure 1. Experimental geometries of **2**–**5** are also given. It is worthwhile to discuss the geometrical data in more detail because the calculated and experimental results already provide valuable information about the bonding situation of the molecules. Unless otherwise noted, we use the BP86/TZ2P values for the discussion.

The calculated bending angle in parent CDP **1** (125.1°) becomes more obtuse in hexamethyl- and hexaphenyl-substituted homologues **2** (136.9°) and **3** (136.9°). The experimental value for **3** (131.7(3)°), obtained from X-ray structure analysis,[10b] is in good agreement with the calculated value, and so is the experimental value for the central P–C bond length (1.635(5) Å), which is slightly shorter than the theoretical datum (1.652 Å). Donor–acceptor bonds become shorter in the solid state,[53] which explains the difference between the calculated and measured values. Noteworthy is the rather large discrepancy between the theoretical and ex-

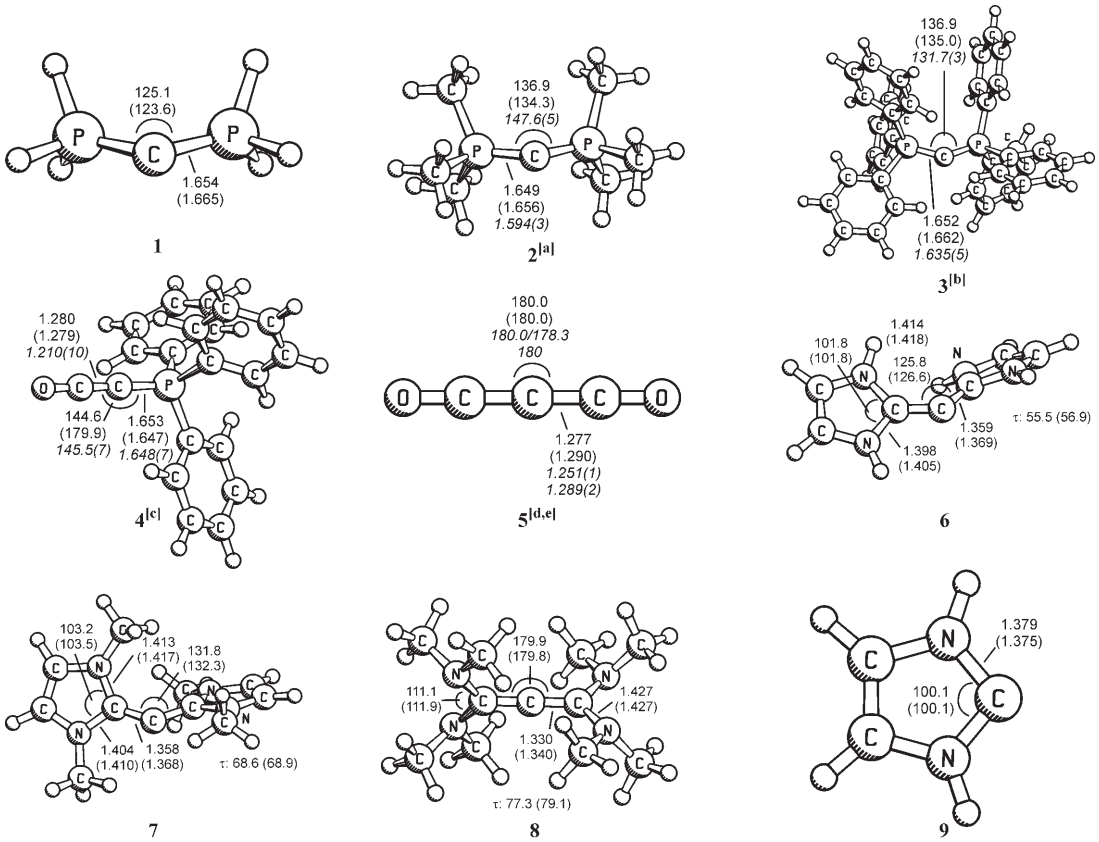

Figure 1. Optimized geometries (bond lengths [Å], angles [°]) at the BP86/TZ2P level(BP86/SVP) of **1**–**9**. Experimental values are given in italics. [a] Experimental values from electron diffraction taken from ref. [54]. [b] Experimental values from X-ray analysis taken from ref. [10b]. [c] Experimental values from X-ray analysis taken from ref. [24]. [d] Experimental values (top) from X-ray analysis taken from ref. [60]. [e] Experimental values (bottom) from electron diffraction taken from ref. [59].

perimental values for **2**. The latter data were obtained from gas-phase electron diffraction[54] and should therefore be in better agreement with theoretical values. We reoptimized the geometry of **2** at the BP86 level using larger basis sets and at the MP2 level using a TZVP basis set. The calculated P–C distances vary between 1.644 (BP86/TZV3P) and 1.660 Å (MP2/TZVP). We think that the experimental value for the central P–C bond length of **2** is too long and that the measured P-C-P bond angle is too large. The calculations predict that **2** and **3** have the same P-C-P angle of 136.9°. The electron diffraction result for $Me_3P{=}CH_2$ obtained by the same group[55] has been questioned by Rankin and coworkers.[56] It was concluded in the latter study that the P–C bond length was too short in the earlier examinations due to too stringent assumptions during the refinement procedure. Thus, it can be assumed that similar problems occurred for the measurement of **2** and that the experimentally determined bond length of this compound is probably too short.

The bending potential for the P-C-P angle of the CDPs is not very deep. We calculated the energy which is necessary to stretch the P-C-P angle to 180°. Table 1 shows that the energy differences between the equilibrium structure and the linear forms of **1**–**3** are not very large. The slightly larger value for **3** ($\Delta E = 3.1$ kcal mol^{-1}) than for **2** ($\Delta E =$ 0.9 kcal mol^{-1}) suggests that the bending potential is mainly determined by subtle changes in the R_3P-C-PR_3 bonding situation but not by steric interactions between the PR_3 groups. The bending potential becomes extremely shallow when one PPh_3 group of **3** is substituted by a CO ligand yielding **4**. Figure 1 shows that the calculated bending angle of **4** at the BP86/TZ2P level[57] is 144.6°, which is in very good agreement with the experimental result from X-ray structure analysis (145.5(7)°).[24] Geometry optimization with

Table 1. Calculated (BP86/TZ2P) relative energies [kcal mol^{-1}] of **1**–**8** with different bending angles α.

$L^1 \overset{C}{\underset{\alpha}{\smile}} L^2$

L^1	L^2	No.	Equilibrium structure	$\alpha = 180°$	$\alpha = 136.9°$
PH_3	PH_3	**1**	0.0	2.0	0.3
PMe_3	PMe_3	**2**	0.0	0.9	0.0
PPh_3	PPh_3	**3**	0.0	3.1	0.0
PPh_3	CO	**4**	0.0	0.3	0.5
CO	CO	**5**	0.0	0.0	1.9
NHC_H	NHC_H	**6**	0.0	3.6	0.6
NHC_{Me}	NHC_{Me}	**7**	0.0	3.2	0.1
$C(NMe_2)_2$	$C(NMe_2)_2$	**8**	0.0	0.0	5.3

a smaller basis set at the BP86/SVP level gives a nearly linear OC-C-P angle of 179.9°. The energy difference at the BP86/TZ2P level between the equilibrium geometry of **4** and the structure in which the OC-C-P angle is frozen at 180.0° is only 0.3 kcal mol^{-1} (Table 1). The linear form resembles the structure of a ketene and the trivial name for compound **4** is actually phosphoranylideneketene.[24] The bonding analysis given below suggests that **4** should better be termed either carbonylcarbophosphorane or carbocarbonylphosphorane.[58]

The experimental value for the C–CO bond length of **4** in the solid state (1.210(10) Å)[24] is significantly smaller than the calculated value (1.280 Å). We think that the difference between the theoretical and experimental value is at least partly due to intermolecular interactions in the crystal, which can yield significantly shorter interatomic distances for donor–acceptor bonds.[53] This conjecture is supported by the experimental values for the C–CO distance of C_3O_2 (**5**) which are available from electron diffraction (1.289(2) Å)[59] and X-ray structure analysis (1.251(1) Å).[60] The gas-phase value is in good agreement with the calculated C–CO bond length (1.277 Å), while the value for the solid-state structure is clearly smaller. Electron diffraction and X-ray measurements show that **5** has a linear (180.0°) or nearly linear (178.3°) OC-C-CO angle. The calculations also give a linear ($D_{\infty h}$) geometry for C_3O_2 but the bending potential is very shallow. The energy which is necessary to distort the linear form of **5** to an OC-C-CO angle of 136.9° (i.e., the equilibrium L-C-L angle of **3**) is only 1.9 kcal mol^{-1}. Previous high-level ab initio calculations on carbon suboxide already showed that the bent form is even slightly lower in energy if the geometry optimization is carried out at the CCSD(T) level of theory.[27]

The equilibrium geometries of the carbodicarbenes **6** and **7** exhibit even more acute bond angles at the divalent carbon atom than CDPs **2** and **3** (Figure 1). The NHC→C donor–acceptor bonds are rather short; the values for **6** (1.359 Å) and **7** (1.358 Å) are in the range of a typical C–C double bond. The NHC ligands are twisted with respect to the central C-C-C plane by 27.8 (**6**) and 34.3° (**7**). Rotation of the NHC ligands about the C–C bond has low energy barriers. Figure 2 shows calculated structures and relative energies of **6** which have been optimized with symmetry constraints. The calculated values for methyl-substituted homologue **7** are given in parentheses.

The NHC ligands in structures **6a** and **7a** are perpendicular to each other, while structures **6b** and **7b** are planar. The energy differences of the perpendicular species with respect to the equilibrium geometries are only 2.3 kcal mol^{-1} for **6a** and 2.1 kcal mol^{-1} for **7a**. Note that the central C–C bonds become significantly shorter in the perpendicular species, which are higher order saddle points on the potential-energy surfaces (Figure 2). The planar form **6b** is only 3.3 kcal mol^{-1} higher in energy than **6**, while methyl-substituted planar homologue **7b** is 12.6 kcal mol^{-1} less stable than **7**. The larger energy difference between the latter species probably comes from steric repulsion between the

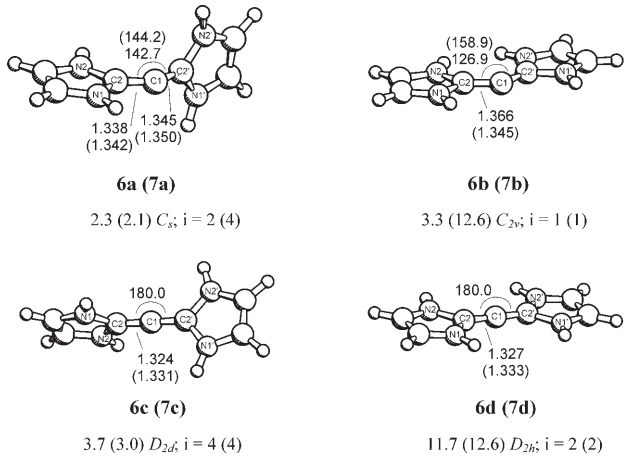

Figure 2. Optimized geometries and relative energies [kcal mol^{-1}] at the BP86/TZ2P level of carbodicarbene **6** with restrained angles: **6a** has perpendicular NHC planes, **6b** has a planar geometry, **6c** has perpendicular NHC planes and a linear arrangement of the central C-C-C moiety and **6d** has a planar geometry and a linear arrangement of the central C-C-C moiety. Relative energies are given with respect to the equilibrium geometry **6** (Figure 1). The number of imaginary frequencies is given by *i*. Results for the structures of the *N*-methyl-substituted carbodicarbene **7** are given in parentheses.

methyl groups. Note that steric repulsion in **7b** enforces a significantly larger bending angle at the central carbon atom (158.9°) compared with the equilibrium structure **7** (131.8°), while the central C–C bond length in **7b** (1.345 Å) is even shorter than in **7** (1.358 Å). The bending potential for the dicarbenes with perpendicular NHC ligands is rather shallow. The linear forms **6c** and **7c** are only 3.7 (**6c**) and 3.0 kcal mol^{-1} (**7c**) higher in energy than the equilibrium structures. The planar forms **6d** and **7d**, which also have a linear C-C-C arrangement, are 11.7 (**6d**) and 12.6 kcal mol^{-1} (**7d**) less stable than the energy minima.

The central N_2C-C-CN_2 moiety of carbodicarbenes **6** and **7** is the same as in tetraaminoallenes (TAAs) $(R_2N)_2C{=}C{=}C(NR_2)_2$. The last-named compounds are experimentally known and their reactivity and properties were studied many years ago.[61] Unfortunately, there is no experimentally determined geometry of a free TAA known to us. Figure 1 shows the optimized geometry of the *N*-methyl-substituted TAA $(Me_2N)_2C{=}C{=}C(NMe_2)_2$ (**8**). Contrary to carbodicarbenes **6** and **7**, the central carbon atoms of **8** have a quasi-linear arrangement with a C-C-C bond angle of 179.9°. Calculations on the ethyl homologue $(Et_2N)_2C{=}C{=}C(NEt_2)_2$ gave a bond angle of only 169.5°, which indicates a shallow bending potential for TAAs.[30] Table 1 shows that the optimized structure of **8** in which the C-C-C angle is constrained to 136.9° is only 5.3 kcal mol^{-1} higher in energy than the linear equilibrium form. The strength of the bending potential of the allene moiety is significantly weakened by the amino substituents. Calculations on the parent allene $H_2C{=}C{=}CH_2$ at the BP86/TZ2P level predict an energy difference between the linear (D_{2d}) energy minimum and the optimized structure in which the C-C-C angle is constrained to 136.9° to be 16.3 kcal mol^{-1}. Figure 1 also shows the optimized ge-

ometry of the parent NHC compound **9**. Note that the N–$C_{carbene}$ bonds of the NHC species (bond length in the free species 1.379 Å) are no longer degenerate in the carbodicarbenes; they are clearly longer in **6** (1.398 and 1.414 Å) and **7** (1.404 and 1.413 Å).

An important question is the strength of the carbon–ligand bonds in compounds **1–9**. To this end we calculated the bond dissociation energies of reaction (5) where L^1 and L^2 are identical except for **4** (L^1=CO, L^2=PPh_3) and **9** (L^1-L^2=HN=CH–CH=NH).

$$CL^1L^2 \rightarrow C(^3P) + L^1 + L^2 \quad (5)$$

Note that reaction (5) is spin-symmetry-forbidden because the ligands L have a singlet ground state while the carbon atom has a triplet ground state. Table 2 lists the calculated bond dissociation energies (BDEs) at various levels of theory.

Table 2. Dissociation energies D_e and energies including thermal and vibrational contributions D_0^{298} for the dissociation reaction $C(L^1L^2)\rightarrow C(^3P)+L^1+L^2$. Geometries were optimized at the BP86/SVP level. All energies [kcal mol^{-1}] were calculated with the TZVPP basis set.

			BP86		MP2		SCS-MP2		CCSD(T)		Exptl
L^1	L^2	No.	D_e	D_0^{298}	D_e	D_0^{298}	D_e	D_0^{298}	D_e	D_0^{298}	D_0^{298}
PH_3	PH_3	**1**	107.8	103.4	108.7	104.2	100.6	96.1	93.3	88.8	–
PMe_3	PMe_3	**2**	135.8	132.3	145.3	141.8	134.6	131.1	129.0	125.5	–
PPh_3	PPh_3	**3**	129.9	126.4	151.3	147.8	137.7	134.2	–	–	–
PPh_3	CO	**4**	161.7	157.4	156.6	152.3	145.4	141.1	–	–	–
CO	CO	**5**	175.7	170.8	154.8	149.8	142.3	137.3	136.0	131.1[a]	140.9[b]
NHC_H	NHC_H	**6**	178.4	175.2	174.7	171.5	165.8	162.6	160.4	157.2	–
NHC_{Me}	NHC_{Me}	**7**	178.9	175.2	181.5	177.7	170.3	166.5	–	–	–
$C(NMe_2)_2$	$C(NMe_2)_2$	**8**	202.8	198.1	219.2	214.5	208.0	203.3	–	–	–
HN=CH–CH=NH		**9**	171.8	168.1	170.4	166.7	161.5	157.8	158.6	154.9	–

[a] The CCSD(T) value extrapolated to the basis set limit is 136.5 kcal mol^{-1}. [b] Ref. [64].

The theoretically predicted BDEs for reaction (5) are quite large. A comparison of the calculated values at the different levels of theory shows that the BP86/TZVPP and MP2/TZVPP values are too high for most molecules. This becomes obvious by comparing the data with the CCSD(T)/TZVPP and SCS-MP2/TZVPP results, which are used as reference values. It has been shown before that the SCS-MP2 method gives energies which are in much better agreement with experimental values than the standard MP2 approximation.[62] From Table 2 it can be seen that the SCS-MP2/TZVPP data are roughly 6 kcal mol^{-1} larger than the CCSD(T)/TZVPP values of **1**, **2**, **5**, and **6**, while the MP2/TZVPP values show much larger deviations from the results which are obtained by using the CCSD(T)/TZVPP method. The only experimental data given in Table 2 is the ΔD_0^{298} value of C_3O_2, which was calculated as the difference between the measured heats of formation ΔH_f^{298} of C_3O_2, CO and $C(^3P)$.[63] The CCSD(T)/TZVPP value (131.1 kcal mol^{-1}) is somewhat smaller than the experimental result (140.9 kcal mol^{-1}). Extrapolation to the basis-set limit for CCSD(T) gives a BDE of 136.5 kcal mol^{-1}, which is in reasonable agreement with experiment.

The theoretical BDEs of **1–9** (Table 2) at all levels of theory indicate that carbodicarbenes **6** and **7** have much stronger bonds than CDPs **1–3**. The SCS-MP2/TZVPP data suggest that substitution of one PPh_3 group in **3** by CO gives a larger total bond energy in **4** (D_e=145.4 kcal mol^{-1}) than in **3** (D_e=137.7 kcal mol^{-1}), but replacing the second PPh_3 ligand by CO yielding **5** slightly weakens the bonds (D_e=142.3 kcal mol^{-1}). The PPh_3 and CO ligands apparently have a synergistic effect on the total bond energy of the carbon atom. The highest bond energy at all levels of theory is calculated for TAA **8**.

Our previous studies strongly suggest that the chemical bonding in CDPs **1–3** and carbodicarbenes **6** and **7** should be discussed in terms of donor–acceptor interactions L→C←L (L=PR_3, NHC).[9,30] The interacting fragments in these species are the donor ligands L and the acceptor carbon atom in the electronic singlet states. The appropriate electronic state of the carbon atom is ^1D, which is 29.1 kcal mol^{-1} higher in energy than the ^3P state.[64] We calculated the strength of the donor–acceptor interactions in CL_2 by taking the BDE values D_e given in Table 2 and adding the $C(^3P)\rightarrow C(^1D)$ excitation energy, which gives the donor–acceptor bond strength D_e for two $L\rightarrow C(^1D)$ bonds. Table 3 lists the theoretically estimated D_e values for one $L\rightarrow C(^1D)$ bond in **1–3** and **5–8**. Compound **8** was included in the calculations because the chemical properties and the analysis of the bonding situation which is given below indicates that TAA **8** can be considered as a "masked" donor–

Table 3. Theoretically estimated strength of the $L\rightarrow C(^1D)$ and $L\rightarrow BH_3$ donor–acceptor bonds [kcal mol^{-1}]. The values were calculated by using one half of the D_e values from Table 2, which are corrected by the excitation energy $C(^3P)\rightarrow C(^1D)$ (29.1 kcal mol^{-1}). The geometries were optimized at the BP86/SVP level. All energies were calculated with the TZVPP basis set.

		$L\rightarrow C(^1D)$				$L\rightarrow BH_3$			
L	No.	BP86	MP2	SCS-MP2	CCSD(T)	BP86	MP2	SCS-MP2	CCSD(T)
PH_3	**1**	68.5	68.9	64.9	61.2	28.0	26.5	22.7	24.0
PMe_3	**2**	82.4	87.2	81.9	79.1	41.5	42.0	37.5	39.5
PPh_3	**3**	79.5	90.2	83.4	–	36.7	38.7	34.3	–
CO	**5**	102.4	91.9	85.7	82.5	37.8	26.6	21.6	23.8
NHC_H	**6**	103.8	101.9	97.4	94.7	58.6	57.3	53.2	54.9
NHC_{Me}	**7**	104.0	105.3	99.7	–	59.1	59.4	54.7	–
$C(NMe_2)_2$	**8**	115.9	124.1	118.5	–	57.5	59.5	54.4	–

acceptor compound. For comparison we also give the calculated bond strength D_e of the analogous complexes L→BH_3.

The results shown in Table 3 suggest that the L→C(^{1}D) bonds in **1–3** and in **5–8** are quite strong. The calculated bond energies for the L→C(^{1}D) bonds are roughly twice as large as the values for the respective L→BH_3 bond. The NHC ligands are clearly stronger donors than phosphines PR_3 with respect to both C(^{1}D) and BH_3 as Lewis acid. The strong Lewis basicity of diaminocarbenes has already been reported.[65] The large value for the OC→C(^{1}D) bond is at first sight surprising and may be taken as a hint that the interpretation of C_3O_2 as a donor–acceptor complex is not justified. We note, however, that MP2 and CCSD(T) calculations indicate that CO and PH_3 are equally strong Lewis bases with respect to BH_3. There is no absolute scale for the strength of a Lewis acid or Lewis base; rather, it depends on the particular binding partners, which can significantly change the order of the donor–acceptor bond strength. A dramatic example was recently reported for the compounds H_3B–L and H_2B^+–L (L=CO, EC_5H_5; E=N–Bi).[66] The calculated BH_3–CO bond is stronger than the H_3B–EC_5H_5 bonds for E=N–Bi, but the binding interactions in H_2B^+–EC_5H_5 are much stronger than in H_2B^+–CO. It is well known that π backdonation plays an important role in the donor–acceptor strength of carbonyl complexes.[67] C(^{1}D) is a strong π donor and σ acceptor which induces strong OC→C(^{1}D) σ donation and OC←C(^{1}D) π backdonation. The latter interaction explains why the OC→C(^{1}D) interaction is nearly as strong as NHC_H→C(^{1}D) and NHC_{Me}→C(^{1}D) bonding, while the OC→BH_3 interaction is only half as strong as NHC_H→BH_3 and NHC_{Me}→BH_3 bonding (Table 3). We show below that π backdonation in **6** and **7** is significantly stronger than in OC→BH_3.

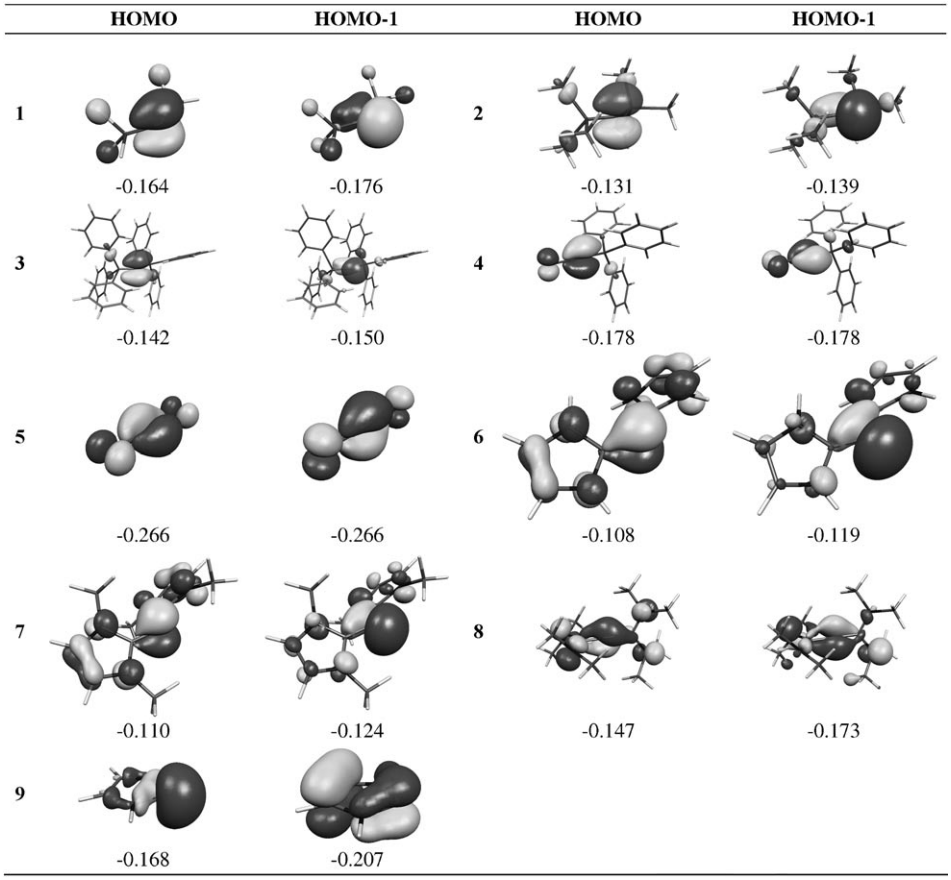

Figure 3. Shape and eigenvalues [eV] of the two highest lying occupied orbitals HOMO and HOMO−1 of **1–9** at the BP86/SVP level.

Bonding analysis: We analyzed the bonding situation in compounds **1–9** using charge- and energy-decomposition methods. Figure 3 shows the two highest lying occupied orbitals of the molecules. The numerical results of the NBO analysis are given in Table 4. Figure 4 shows a sketch of the most favorable Lewis structures given by the NBO calculations, in which three-center delocalized orbitals were allowed for but were unfavorable in all cases.

Table 4. NBO results (BP86/TZVPP//BP86/SVP) for **1–9**. Partial charges q and orbital populations are given in electrons.

L^1	L^2	No.	q(C)[a]	q(E)[b]	LP(C)$_\sigma$[a] Occ[d]	LP(C)$_\sigma$[a] %[d]	LP(C)$_\pi$[a] Occ[d]	Residual density [%][c,d]
PH_3	PH_3	**1**	−1.32	0.78	1.62	42.6	1.51	2.5
PMe_3	PMe_3	**2**	−1.47	1.53	1.60	25.7	1.53	1.4
PPh_3	PPh_3	**3**	−1.43	1.52	1.59	26.4	1.52	3.1
PPh_3	CO	**4**	−0.96	1.54/0.58	(1.37)	(0.0)	(1.37)	3.2 (3.3)
CO	CO	**5**	−0.55	0.65	(1.25)	(0.0)	(1.25)	4.8 (4.8)
NHC_H	NHC_H	**6**	−0.51	0.28	(1.51)	(6.4)	(1.11)	2.8 (4.2)
NHC_{Me}	NHC_{Me}	**7**	−0.50	0.29	(1.45)	(5.7)	(1.16)	2.3 (3.3)
$C(NMe_2)_2$	$C(NMe_2)_2$	**8**	−0.21	0.25	(1.14)	(0.0)	(1.10)	1.4 (2.9)
HN=CH–CH=NH		**9**	0.04	−0.53	1.91	51.7	(0.67)	2.5 (5.1)

[a] Central carbon atom. [b] Atom E which is directly bonded to the central carbon atom. For **1–3**: E=P, for **4**: E=P/C, for **5–8**: E=C; for **9**: E=N. [c] Density that is left after the diagonalization step resulting in the NBOs. Given as total non-Lewis contribution in the NBO calculation. [d] Values in parentheses come from Lewis structures with two lone pairs at the central carbon atom which have been enforced in the NBO calculations.

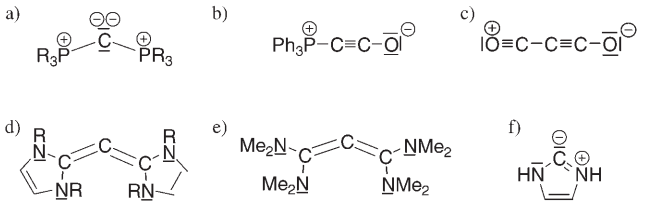

Figure 4. Most favorable Lewis structures for **1**–**9** given by the NBO method. Only one of two equivalent Lewis structures are shown in c and f.

The shapes of the HOMO and HOMO−1 of CDPs **1**–**3** clearly reveal the lone-pair character of the orbitals (Figure 3). The σ-type lone-pair orbital is always slightly lower in energy than the π-type lone-pair orbital which is the HOMO of the CDPs. Note that the small contributions at the PR_3 groups in the HOMO and HOMO−1 stem from σ*(P−R) orbitals which stabilize the high electron density at the central carbon atom by negative hyperconjugation. The lone-pair character of these frontier orbitals is quantitatively supported by the NBO results (Table 1), which suggest that the HOMO and HOMO−1 are carbon lone-pair MOs occupied by about 1.5–1.6 electrons. The NBO analysis suggests that the most favorable Lewis structures of **1**–**3** should be written as shown in Figure 4a. The interpretation of the electronic structure in terms of two lone-pair MOs is also in agreement with the calculated charge distribution, which indicates that the two-coordinate carbon atom in the CDPs carries a large negative charge of between −1.32e (**1**) and −1.47e (**2**).

Substitution of PPh_3 in $C(PPh_3)_2$ (**3**) by CO significantly reduces the negative charge at carbon to −0.96e in (CO)C-(PPh_3) (**4**) and to −0.55e in $C(CO)_2$ (**5**). The default NBO calculations do not give lone-pair orbitals at the central carbon atom. Instead, the best Lewis structure of carbon suboxide is degenerate and has alternating single and triple bonds ($O^-{-}C{\equiv}C{-}C{\equiv}O^+$) rather than double bonds, while (CO)C(PPh_3) is calculated as $Ph_3P^+{-}C{\equiv}C{-}O^-$ (Figure 4b and c). Figure 3 shows that the orbital contributions from CO to the HOMO and HOMO−1 of **4** and **5** are clearly larger than the ligand-atom contributions in **1**–**3**, but the fact that the largest coefficients are still calculated for the central carbon atom indicates some lone-pair character for the occupied frontier orbitals. We note that the HOMO and HOMO−1 of **4** and **5** have a node between the carbon atoms and the oxygen atoms which indicates an overlap with σ*(L−R) orbitals, as in **1**–**3**. NBO calculations on **4** and **5** in which Lewis structures with two lone-pair orbitals at the carbon atom are enforced give comparable residual densities (Table 4) to the unconstrained NBO calculations.

The NBO calculations on the carbodicarbenes **6** and **7** also do not give carbon lone-pair orbitals at the central carbon atoms (Table 4). Rather, a bonding situation like in an allene with two double bonds (C=C=C) is depicted (Figure 4d), but on looking at the frontier orbitals the coefficients at the central carbon atom are larger than those of the terminal atoms. Figure 3 also reveals significant contributions from unoccupied NHC-ligand AOs which stabilize the orbitals of the two-coordinate carbon atom in the occupied frontier orbitals of **6** and **7**. Table 4 shows that the atomic partial charges at the central carbon atom (−0.51e in **6** and −0.50e in **7**) are comparable to that of carbon suboxide (**5**). Thus, the NBO calculations indicate that the carbodicarbenes have less carbon lone-pair character than the CDPs. Note, however, that the energy levels of the HOMO and HOMO−1 of **6** and **7** are clearly higher than those of **1**–**4** and particularly higher than the HOMO and HOMO−1 of **5**, which means that they are energetically more accessible. NBO calculations on **6** and **7** with enforced σ-and π-type lone-pair orbitals at the central carbon atom gave only a slightly higher residual density than the default calculations, but the differences are larger than for **4** and **5** (Table 4).

As expected, NBO calculations on TAA **8** do not give carbon lone-pair orbitals at the central carbon atom but rather two double bonds (C=C=C, Figure 4e). The atomic partial charge at the central carbon atom of −0.21e is the smallest for compounds **1**–**8** (Table 4). Figure 3 shows, however, that the largest contribution to the highest lying occupied orbitals comes from the two-coordinate carbon atom. The NBO calculation on **8** with enforced σ and π lone pairs at carbon gives only a slightly higher residual density compared with the unconstrained calculation, which points to the "hidden double-lone-pair character" of the TAA which becomes evident in the product of the reaction with CO_2.[61]

The shapes of the HOMO and HOMO−1 of NHC **9** are very interesting (Figure 3). The HOMO is clearly a σ-type lone-pair orbital at the carbene carbon atom, which means that there is a local area of negative charge at the carbon atom in the σ direction. Nevertheless, the carbon atom carries an overall slightly positive partial charge. This is similar to the charge distribution in CO, where the carbon atom is positively charged but behaves like a nucleophile because of the electronic charge of the energetically high lying σ-type lone pair.[2] The NBO calculation gives a Lewis structure (Figure 4f) with an $sp^{0.9}$-hybridized carbon σ-type lone-pair orbital which is occupied by 1.91e (Table 4). Note that the optimal Lewis structures given by the NBO method always have an electron octet, which is preferred over Lewis structures which have the lowest formal charges. The HOMO−1 of **9** is a delocalized π orbital which has large coefficients at the C−C π bond of the NHC ring. The NBO calculation with enforcement of two carbon lone-pairs gives a substantially larger residual density than the default calculation (Table 4).

The results of the charge analysis with the NBO method are nicely complemented by the AIM results of the compounds. Figure 5 shows a contour line diagram of the Laplacians of **1** and **9**. The results for the other compounds are not given since they do not reveal significant new information. It is sufficient to present the Laplacians of **1** and **9** because they are typical for a divalent carbon(0) compound and a divalent carbon(II) molecule.

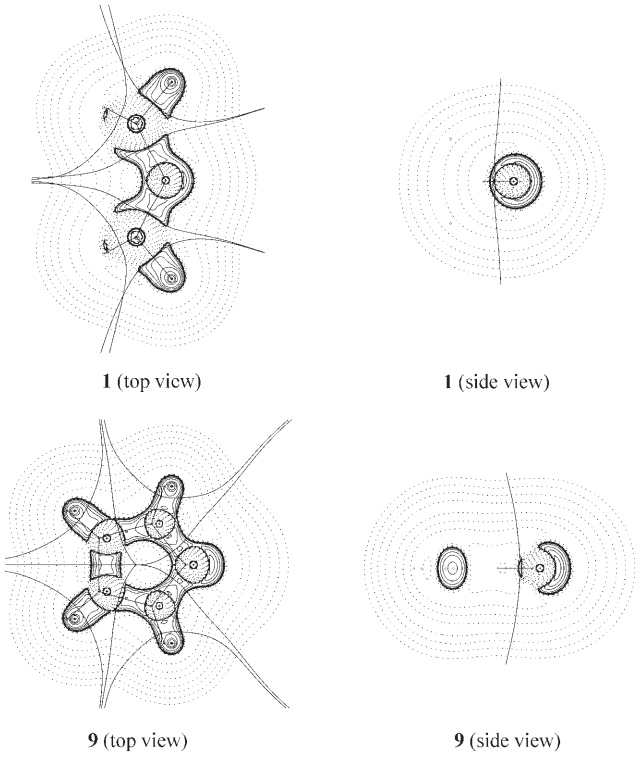

Figure 5. Contour line diagrams $\nabla^2\rho(r)$ of carbodiphosphorane **1** and NHC **9** in two different views. Solid lines indicate areas of charge concentration ($\nabla^2\rho(r)<0$), while dashed lines show areas of charge depletion ($\nabla^2\rho(r)>0$). The thick solid lines connecting the atomic nuclei are the bond paths. The thick solid lines separating the atomic basins indicate the zero-flux surfaces crossing the molecular plane.

The shape of the contour line diagrams of the Laplacian of **1** and **9** in the molecular plane (top view) clearly shows the region of the σ-electron lone pair, which appears as a region of charge concentration ($\nabla^2\rho(r)<0$, solid lines). The droplet-like appendix at the carbon atom of **9** has a larger extension than in **1**, which indicates that the density in the latter has a larger slope at the carbon atom than in the former. The difference in electron configuration at the carbon atoms of **1** and **9** becomes obvious when the Laplacians of the two compounds in the side view (Figure 5) are compared. There is a continuous area of charge concentration around the carbon atom of **1** which comes from the electron density of the σ and π lone pairs. The side view of the Laplacian of **9** is clearly different from that of **1**. There is a hole in the Laplacian distribution which indicates an area of charge depletion in the π direction at the divalent carbon atom of the NHC.

We also analyzed the nature of the carbon–ligand interactions in **1**–**9** by energy decomposition analysis (EDA) with L_2 and C as interacting fragments. The choice of the electron configuration of the carbon atom is crucial for the interpretation of the C–L bonding. EDA calculations on parent CDP **1** and NHC **9** as examples of divalent carbon(0) and carbon(II) compounds, respectively, were carried out with two doubly occupied valence orbitals and two vacant orbitals at the carbon atom in which all possible permutations of the orbital populations were considered. Figure 6a schematically shows the carbon valence orbitals and the

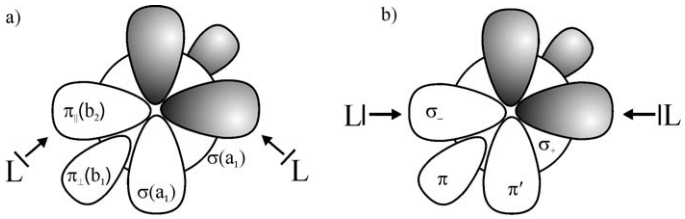

Figure 6. Symmetry assignments for the carbon valence orbitals in a) C_{2v} symmetry and b) in structures **5** and **8** which have a linear C-C-C moiety.

symmetry assignments which were used for structures **1**–**4**, **6**, **7** and **9** for which EDA calculations were carried out under C_{2v} symmetry constraints. The equilibrium structures of some molecules have lower symmetry, but the energy differences between the C_{2v} structures and the fully optimized geometries are not very large and should not impair the bonding analysis. Compounds **5** ($D_{\infty h}$) and **8** (D_{2d}) have linear C-C-C arrangements. The orbital contributions from the different irreducible representations of the respective point group were transformed into σ- and π-bonding interactions, as shown in Figure 6b.

Tables 5 and 6 list the EDA results for **1** and **9** for six different electron configurations (a)–(f) at the carbon atom which are denoted as $C(2s^n2p_\sigma{}^n2p_{\pi\perp}{}^n2p_{\pi\parallel}{}^n)$ where n is 0 or 2. Note that the ligands $(PH_3)_2$ and HN=CH−CH=NH, which are the fragments for the EDA of **1** and **9**, respectively, are in an electronically excited state in schemes (b), (c), (e) and (f). The calculated values reveal interesting details about the bonding situation and they show significant differences between the two compounds. The calculated values for the orbital interactions ΔE_{orb} can be used as an indicator for the best description of the carbon-ligand interactions. Those EDA calculations which give the smallest ΔE_{orb} value indicate which fragments are the best choice for describing the bonding situation, because the least alteration of the electronic charge distribution is required to yield the electronic structure of the molecule. The values in Table 5 show that fragmentation scheme (d) gives the smallest ΔE_{orb} value (-552.7 kcal mol^{-1}) for **1**. The fragments in this scheme are the $(PH_3)_2$ ligand in the electronic ground state and a carbon atom which has one p(σ) and one p($\pi_\perp$) lone-pair orbitals. The result of the energy decomposition thus agrees with the results of the charge analysis given above. Note that the ΔE_{orb} value for fragmentation scheme (a), in which the valence s orbital is occupied instead of the p(σ) orbital, is only slightly higher in energy (-567.8 kcal mol^{-1}) than in fragmentation scheme (d). Nearly the same ΔE_{orb} value as in scheme (a) is calculated for fragmentation scheme (c) (-567.5 kcal mol^{-1}), in which the 2s valence orbital is occupied and the lone-pair electron resides in a p(σ) orbital. The latter fragmentation scheme describes the bonding situation

Table 5. EDA (BP86/TZ2P) with six different partitioning schemes (a)–(f) for **1**. Energies are given in kcal mol^{-1}. See Figure 6 for explanation of the orbital terms. The most favorable partitioning scheme (d) yielding the smallest ΔE_{orb} value is given in italics.

$H_3P^{\diagup C \diagdown}PH_3$

Partition scheme	(a)		(b)		(c)		(*d*)		(e)		(f)	
Electronic state of C atom	$s^2p_\sigma^0p_{\pi\perp}^2p_{\pi\parallel}^0$		$s^2p_\sigma^0p_{\pi\perp}^0p_{\pi\parallel}^2$		$s^2p_\sigma^2p_{\pi\perp}^0p_{\pi\parallel}^0$		$s^0p_\sigma^2p_{\pi\perp}^2p_{\pi\parallel}^0$		$s^0p_\sigma^2p_{\pi\perp}^0p_{\pi\parallel}^2$		$s^0p_\sigma^0p_{\pi\perp}^2p_{\pi\parallel}^2$	
ΔE_{int}	−168.4		−365.9		−503.9		*−552.4*		−749.9		−741.8	
ΔE_{Pauli}	633.8		911.1		209.2		*204.2*		473.2		344.5	
ΔE_{elstat}[a]	−234.4	(29.2)	−561.1	(43.9)	−145.6	(20.4)	*−203.9*	(*26.9*)	−522.0	(42.7)	−446.5	(41.1)
ΔE_{orb}[a]	−567.8	(70.8)	−715.8	(56.1)	−567.5	(79.6)	*−552.7*	(*73.1*)	−701.2	(57.3)	−639.8	(58.9)
$\Delta E_\sigma(a_1)$[b]	−317.9	(56.0)	−317.1	(44.3)	−187.0	(32.9)	*−300.9*	(*54.4*)	−302.5	(43.1)	−362.7	(56.7)
$\Delta E_\delta(a_2)$[b]	−1.1	(0.2)	−0.4	(0.1)	−0.8	(0.1)	*−1.2*	(*0.2*)	−0.3	(0.0)	−0.4	(0.1)
$\Delta E_{\pi\perp}(b_1)$[b]	−60.8	(10.7)	−191.8	(26.8)	−199.1	(35.1)	*−73.7*	(*13.3*)	−177.4	(25.3)	−67.0	(10.5)
$\Delta E_{\pi\parallel}(b_2)$[b]	−188.0	(33.1)	−206.5	(28.8)	−180.6	(31.8)	*−176.9*	(*32.0*)	−221.0	(31.5)	−209.7	(32.8)
ΔE_{prep}	63.9		261.2		399.3		*448.2*		645.5		637.0	
ΔE_{prep}(C)	43.5		43.5		43.6		*427.8*		427.8		427.4	
$\Delta E_{prep}(L_2)$	20.4		217.7		355.8		*20.4*		217.7		209.6	
ΔE ($=-D_e$)	−104.5		−104.7		−104.6		*−104.3*		−104.4		−104.8	

[a] The values in parentheses are the percentage contributions to the total attractive interactions $\Delta E_{elstat}+\Delta E_{orb}$. [b] The values in parentheses are the percentage contributions to the total orbital interactions ΔE_{orb}.

Table 6. EDA (BP86/TZ2P) with six different partitioning schemes (a)–(f) for **9**. Energies are given in kcal mol^{-1}. See Figure 6 for explanation of the orbital terms. The most favorable partitioning scheme (c) yielding the smallest ΔE_{orb} value is given in italics.

Partition scheme	(a)		(b)		(*c*)		(d)		(e)		(f)	
Electronic state of C atom	$s^2p_\sigma^0p_{\pi\perp}^2p_{\pi\parallel}^0$		$s^2p_\sigma^0p_{\pi\perp}^0p_{\pi\parallel}^2$		$s^2p_\sigma^2p_{\pi\perp}^0p_{\pi\parallel}^0$		$s^0p_\sigma^2p_{\pi\perp}^2p_{\pi\parallel}^0$		$s^0p_\sigma^2p_{\pi\perp}^0p_{\pi\parallel}^2$		$s^0p_\sigma^0p_{\pi\perp}^2p_{\pi\parallel}^2$	
ΔE_{int}	−280.7		−336.7		*−468.5*		−664.7		−720.7		−949.0	
ΔE_{Pauli}	691.7		973.6		*463.8*		401.3		671.4		403.7	
ΔE_{elstat}[a]	−292.7	(30.1)	−469.1	(35.8)	*−295.1*	(*31.7*)	−360.2	(33.8)	−527.2	(37.9)	−290.6	(21.5)
ΔE_{orb}[a]	−679.7	(69.9)	−841.2	(64.2)	*−637.3*	(*68.3*)	−705.8	(66.2)	−864.8	(62.1)	−1062.1	(78.5)
$\Delta E_\sigma(a_1)$[b]	−339.0	(49.9)	−332.4	(39.5)	*−386.2*	(*60.6*)	−345.0	(48.9)	−338.6	(39.1)	−445.7	(42.0)
$\Delta E_\delta(a_2)$[b]	−9.6	(1.4)	−3.9	(0.5)	*−8.8*	(*1.4*)	−12.9	(1.8)	−4.6	(0.5)	−2.1	(0.2)
$\Delta E_{\pi\perp}(b_1)$[b]	−175.1	(25.8)	−94.2	(11.2)	*−91.9*	(*14.4*)	−202.7	(28.7)	−78.6	(9.1)	−173.4	(16.3)
$\Delta E_{\pi\parallel}(b_2)$[b]	−155.9	(22.9)	−410.8	(48.8)	*−150.3*	(*23.6*)	−145.2	(20.6)	−443.1	(51.2)	−441.0	(41.5)
ΔE_{prep}	111.0		167.0		*298.9*		495.3		551.3		779.2	
ΔE_{prep}(C)	43.5		43.5		*43.6*		427.8		427.8		427.4	
$\Delta E_{prep}(L_2)$	67.5		123.5		*255.3*		67.5		123.5		351.8	
ΔE ($=-D_e$)	−169.6		−169.6		*−169.6*		−169.4		−169.4		−169.8	

[a] The values in parentheses are the percentage contributions to the total attractive interactions $\Delta E_{elstat}+\Delta E_{orb}$. [b] The values in parentheses are the percentage contributions to the total orbital interactions ΔE_{orb}.

in a singlet carbene. Table 6 shows that the EDA results for NHC **9** give the lowest ΔE_{orb} value for fragmentation scheme (c), which is in agreement with the classification of **9** as a carbene while **1** is a carbon complex.

The ΔE_{orb} value for **1** obtained by using fragmentation scheme (c) in the EDA calculation indicating a carbene-type interaction is not much higher than the ΔE_{orb} value using the fragmentation scheme (d). It is important to realize that the two bonding models are qualitative descriptions which should not be confused with physical reality. The value of the distinction between the two bonding models and the classification of the two compounds in different categories lies in the explanation of the chemical behavior and the predictions which can be made.

In order to directly compare the C–L interactions in **1**–**9** we carried out EDA calculations with the same fragmentation scheme (d) in which the carbon atom has two electron lone pairs. The results for **1**–**8** are given in Table 7. Note that the electron lone pairs in the C_{2v} structures are denoted as p(σ) and p($\pi_\perp$), while in the linear species **5** and **8** they are denoted as p(π) and p(π′), which are degenerate (Figure 6).

The EDA results in Table 7 show that the attractive interactions in the CDPs **1**–**3** mainly come from the orbital term ΔE_{orb}, which contributes 71–73 % to the total attractive interactions ΔE_{int}. The $(R_3P)_2\rightarrow C$ donation into the vacant carbon 2s AO contributes more to the ΔE_{int} term than donation into the p($\pi_\parallel$) AO (see Figure 6a for notation). Note that the stabilization which comes from the $\pi_\perp$ orbitals is rather high (the $\Delta E_{\pi\perp}$ term has values between −68.3 and −73.7 kcal mol^{-1}), which at first sight is surprising because the carbon p($\pi_\perp$) orbital is doubly occupied and the charge analysis suggests that it retains its lone-pair character in the CDPs. The calculated $\Delta E_{\pi\perp}$ values mainly result from hy-

Table 7. EDA (BP86/TZ2P) results of **1**–**8**. All compounds except **4** (C_s), **5** ($D_{\infty h}$), and **8** (D_{2d}) were optimized under C_{2v} symmetry constraints. The interacting fragments of the L_2C compounds are L_2 and C. The carbon fragment is calculated with the electron configuration $C(s^0p_\sigma{}^2p_{\pi\perp}{}^2p_{\pi\parallel}{}^0)$, which is fragmentation scheme (d) in Tables 5 and 6. See Figure 6 for explanation of orbital terms. Energies are given in kcal mol^{-1}.

	1		**2**		**3**		**4**		**5**		**6**		**7**		**8**	
ΔE_{int}	−552.4		−581.4		−575.7		−608.9		−618.5		−644.9		−635.4		−652.5	
ΔE_{Pauli}	204.2		162.8		166.8		153.0		127.8		252.3		180.4		218.0	
ΔE_{elstat}[a]	−203.9	(26.9)	−212.4	(28.5)	−214.8	(28.9)	−175.8	(23.1)	−133.9	(17.9)	−296.9	(33.1)	−248.3	(30.4)	−283.5	(32.6)
ΔE_{orb}[a]	−552.7	(73.1)	−531.9	(71.5)	−527.7	(71.1)	−586.2	(76.9)	−612.4	(82.1)	−600.3	(66.9)	−567.5	(69.6)	−587.1	(67.4)
$\Delta E_\sigma(a_1)$[b]	−300.9	(54.4)	−276.9	(52.1)	−268.4	(50.9)	−486.8[c]	(83.1)			−270.7	(45.1)	−224.8	(39.6)		
$\Delta E_\delta(a_2)$[b]	−1.2	(0.2)	−1.4	(0.3)	−1.8	(0.3)					−10.1	(1.7)	−12.0	(2.1)		
$\Delta E_{\pi\perp}(b_1)$[b]	−73.7	(13.3)	−68.3	(12.8)	−68.7	(13.0)	−99.3[c]	(16.9)			−126.5	(21.1)	−121.6	(21.4)		
$\Delta E_{\pi\parallel}(b_2)$[b]	−176.9	(32.0)	−185.2	(34.8)	−188.8	(35.8)					−193.0	(32.2)	−209.2	(36.9)		
$\Delta E_{\sigma(+)}$[b]									−148.7	(24.3)					−147.5	(25.1)
$\Delta E_{\sigma(-)}$[b]									−225.1	(36.8)					−214.8	(36.6)
ΔE_δ[b]									−16.1	(2.6)					−0.3	(<0.1)
ΔE_π[b]									−111.2	(18.1)					−112.2	(19.1)
ΔE_π[b]									−111.2	(18.1)					−112.2	(19.1)
ΔE_{prep}	448.2		447.8		449.5		448.7		444.9		470.9		468.2		481.6	
$\Delta E_{prep}(C)$	427.8		427.8		427.8		427.9		428.1		427.8		427.8		427.4	
$\Delta E_{prep}(L_2)$	20.4		20.0		21.7		20.8		16.8		43.0		40.4		54.2	
$\Delta E\ (=-D_e)$	−104.3		−133.6		−126.1		−160.3		−173.5		−174.0		−167.2		−170.9	

[a] The values in parentheses are the percentage contributions to the total attractive interactions $\Delta E_{elstat}+\Delta E_{orb}$. [b] The values in parentheses are the percentage contributions to the total orbital interactions ΔE_{orb}. [c] Only C_s-symmetric structure; therefore, $\Delta E_{orb}=\Delta E_\sigma(a')+E_\sigma(a'')$.

perconjugative stabilization of the carbon lone pair by the σ*(P−R) orbitals. The small contributions from the ΔE_δ term arising from the polarisation functions are negligible.

The EDA of **4** was carried out under C_s symmetry constraint, which impedes the distinction between ΔE_σ and $\Delta E_{\pi\parallel}$ interactions. Table 1 shows that the $\pi_\perp$ orbital interactions in **4** are stronger (−99.3 kcal mol^{-1}) than in **1**–**3**; this hints at enhanced C→L $\pi_\perp$ donation due to the low-lying vacant π* orbital of CO. This interpretation is supported by the EDA results for carbon suboxide (**5**). The orbital interactions which come from the degenerate C→$(CO)_2$ π backdonation are even larger ($\Delta E_\pi=\Delta E_{\pi'}=-111.2$ kcal mol^{-1}) than the $\Delta E_{\pi\perp}$ value for **4**. This is in agreement with the NBO analysis, which suggests that the best Lewis structures have C−C multiple bonds. Note that the NBO result is helpful for qualitative interpretation, while the EDA provides a quantitative estimate of the relative strengths of orbital interactions which have different symmetry.

The EDA results for the carbodicarbenes **6** and **7** clearly show that the $\pi_\perp$ orbital interactions become even stronger ($\Delta E_{\pi\perp}=-126.5$ kcal mol^{-1} for **6** and $\Delta E_{\pi\perp}=-121.6$ kcal mol^{-1} for **7**) than in **5**. This is in agreement with the charge analyses, which indicate that the $\pi_\perp$ orbital in the carbodicarbenes is more delocalized than in CDPs **1**–**3** but less delocalized than in carbene **9**. The EDA results for **9** with the same fragmentation scheme as for the other compounds shows indeed that the $\pi_\perp$ orbital interactions are much stronger [$\Delta E_{\pi\perp}=-202.7$ kcal mol^{-1}, Table 6, scheme (d)] than in the other compounds. The calculated values for the $\Delta E_{\pi\perp}$ term can thus be used as a probe for the divalent carbon(0) character of a compound. The EDA results for TAA **8**, which has a linear C-C-C moiety, shows that C→C-$(NMe_2)_2$ π backdonation ($\Delta E_\pi=\Delta E_{\pi'}=-112.2$ kcal mol^{-1}) is comparable to that of C_3O_2 (**5**), which suggests that the divalent carbon(0) character of both compounds is similar. This is in agreement with the calculated properties of main group and transition metal complexes with **5** and **8** as ligands, which are presented and discussed in the following paper.[31]

Conclusion

The theoretical data presented here clearly show that the bonding situations in L_2C compounds **1**–**8** can be interpreted in terms of donor–acceptor interactions between closed-shell ligands L and a carbon atom which has two lone-pair orbitals (L→C←L). This holds particularly for the carbodiphosphoranes **1**–**3** where L = PR_3. The NBO analysis suggests that the best Lewis structures for the carbodicarbenes **6** and **7** where L is a NHC ligand have C=C=C bonds, as in tetraaminoallene **8**. However, the Lewis structures of **6**–**8** in which two lone-pair orbitals at the central carbon atom are enforced have only a slightly higher residual density. Visual inspection of the frontier orbitals of the latter species reveals their high lone-pair character, which suggests that even the quasi-linear TAA **8** is a "masked" divalent carbon(0) compound. This explains the very shallow bending potential of **8**. The same conclusion is made for the phosphoranylketene **4** and for carbon suboxide (**5**), which according to the bonding analysis have a hidden double-lone pair character. The AIM analysis and the EDA calculations support the assignment of carbodiphosphoranes as divalent carbon(0) compounds, while NHC **9** is confirmed as a carbene. The L→C(^{1}D) donor–acceptor bonds are roughly twice as strong as the respective L→BH_3 bond. We emphasize that the description of the bonding situation with different models and terms such as carbon(0) and carbon(II) compounds do not represent physical realities. However, they

are very useful for understanding and predicting the chemical behavior of **1**–**9**, which is discussed in the following paper.[31]

Acknowledgements

This work was supported by the Deutsche Forschungsgemeinschaft. Excellent service by the Hochschulrechenzentrum of the Philipps-Universität Marburg is gratefully acknowledged. Further computer time was provided by the HLRS Stuttgart and HHLRZ Darmstadt.

[1] S. Huzinaga, E. Miyoshi, M. Sekiya, *J. Comput. Chem.* **1993**, *14*, 1440.
[2] For a recent discussion of the electronic structure and bonding situation in CO, see: G. Frenking, C. Loschen, A. Krapp, S. Fau, S. H. Strauss, *J. Comput. Chem.* **2007**, *28*, 117.
[3] a) R. G. Carlson, M. A. Gile, J. A. Heppert, M. H. Mason, D. R. Powell, D. V. Velde, J. M. Vilain, *J. Am. Chem. Soc.* **2002**, *124*, 1580; b) S. R. Caskey, M. H. Stewart, J. E. Kivela, J. R. Sootsman, M. J. A. Johnson, J. W. Kampf, *J. Am. Chem. Soc.* **2005**, *127*, 16750.
[4] For a theoretical analysis of the bonding situation in transition metal carbon complexes, see: a) Y. Chen, W. Petz, G. Frenking, *Organometallics* **2000**, *19*, 2698; b) A. Krapp, K. K. Pandey, G. Frenking, *J. Am. Chem. Soc.* **2007**, *129*, 7596.
[5] A. J. Arduengo, III, R. L. Harlow, M. Kline, *J. Am. Chem. Soc.* **1991**, *113*, 2801.
[6] a) A. Baceiredo, G. Bertrand, G. Sicard, *J. Am. Chem. Soc.* **1985**, *107*, 4781; b) A. Igau, H. Grützmacher, A. Baceiredo, G. Bertrand, *J. Am. Chem. Soc.* **1988**, *110*, 6463; c) A. Igau, A. Baceiredo, G. Trinquier, G. Bertrand, *Angew. Chem.* **1989**, *101*, 617; *Angew. Chem. Int. Ed. Engl.* **1989**, *28*, 621.
[7] W. Kirmse, *Angew. Chem.* **2004**, *116*, 1799; *Angew. Chem. Int. Ed.* **2004**, *43*, 1767.
[8] a) *N-Heterocyclic Carbenes in Synthesis* (Ed.: S. P. Nolan), Wiley-VCH, New York, **2006**; b) *Carbene Chemistry*, (Ed.: G. Bertrand), Marcel Dekker, New York, **2002**.
[9] R. Tonner, F. Öxler, B. Neumüller W. Petz, G. Frenking, *Angew. Chem.* **2006**, *118*, 8206; *Angew. Chem. Int. Ed.* **2006**, *45*, 8038.
[10] a) F. Ramirez, N. B. Desai, B. Hansen, N. McKelvie, *J. Am. Chem. Soc.* **1961**, *83*, 3539; b) G. E. Hardy, J. I. Zink, W. C. Kaska, J. C. Baldwin, *J. Am. Chem. Soc.* **1978**, *100*, 8002.
[11] Recent reviews: a) N. D. Jones, R. G. Cavell, *J. Organomet. Chem.* **2005**, *690*, 5485; b) O. I. Kolodiazhnyi, *Phosphorous Ylides: Chemistry and Application in Organic Synthesis*, Wiley-VCH, Weinheim, **1999**; c) O. I. Kolodiazhnyi, *Tetrahedron* **1996**, *52*, 1855; d) *Ylides and Imines of Phosphorus* (Ed.: A. W. Johnson), Wiley, New York, **1993**.
[12] a) J. I. Zink, W. C. Kaska, *J. Am. Chem. Soc.* **1973**, *95*, 7510; b) J. I. Zink, *Acc. Chem. Res.* **1978**, *11*, 289. The word was coined in G. Wiedemann, F. Schmidt, *Ann. Phys. (Leipzig)*, **1895**, *54*, 604.
[13] W. C. Kaska, D. K. Mitchell, R. F. Reichelderfer, *J. Organomet. Chem.* **1973**, *47*, 391.
[14] W. Petz, C. Kutschera, M. Heitbaum, G. Frenking, R. Tonner, B. Neumüller, *Inorg. Chem.* **2005**, *44*, 1263.
[15] a) J. D. Walker, R. Poli, *Polyhedron* **1989**, *8*, 1293; b) W. P. Jensen, H. Gehrke, D. R. Jones, I.-H. Suh, R. A. Jacobson, *Z. Kristallogr.* **1996**, *211*, 829.
[16] J. Vicente, A. R. Singhal, P. G. Jones, *Organometallics* **2002**, *21*, 5887.
[17] W. Petz, F. Weller, J. Uddin, G. Frenking, *Organometallics* **1999**, *18*, 619.
[18] W. Petz, F. Öxler, B. Neumüller, G. Frenking, R. Tonner, unpublished results.
[19] G. Frenking, N. Fröhlich, *Chem. Rev.* **2000**, *100*, 717.
[20] a) A. J. Lupinetti, G. Frenking, S. H. Strauss, *Angew. Chem.* **1998**, *110*, 2229; *Angew. Chem. Int. Ed.* **1998**, *37*, 2113; b) A. J. Lupinetti, S. H. Strauss, G. Frenking, *Prog. Inorg. Chem.* Vol. 49, p. 1, K. D. Karlin (Ed), Wiley, New York, **2001**.
[21] A. Diefenbach, F. M. Bickelhaupt, G. Frenking, G. *J. Am. Chem. Soc.* **2000**, *122*, 6449.
[22] W. A. Herrmann, *Angew. Chem.* **2002**, *114*, 1342; *Angew. Chem. Int. Ed.* **2002**, *41*, 1290.
[23] R. Tonner, G. Heydenrych, G. Frenking, *Chem. Asian J.* **2007**, *2*, 1555.
[24] J. J. Daly, P. Wheatley, *J. Chem. Soc.* **1966**, 1703.
[25] O. Diels, B. Wolf, *Ber. Dtsch. Chem. Ges.* **1906**, *39*, 689.
[26] a) T. Kappe, E. Ziegler, *Angew. Chem.* **1974**, *86*, 529; *Angew. Chem. Int. Ed. Engl.* **1974**, *13*, 491; b) G. Paiaro, L. Pandolfo, *Comments Inorg. Chem.* **1991**, *12*, 213.
[27] J. Koput, *Chem. Phys. Lett.* **2000**, *320*, 237.
[28] a) W. Grahn, *Liebigs Ann. Chem.* **1981**, 107; b) W Grahn, Habilitation Thesis, University Marburg, **1979**.
[29] N. Kuhn, H. Bohnen, T. Kratz, G. Henkel, *Liebigs Ann. Chem.* **1993**, 1149.
[30] R. Tonner, G. Frenking, *Angew. Chem.* **2007**, *119*, 8850; *Angew. Chem. Int. Ed.* **2007**, *46*, 8695.
[31] R. Tonner, G. Frenking, *Chem. Eur. J.* **2008**, *14*, DOI: 10.1002/chem.200701392.
[32] Gaussian 03, Revision D.01, M. J. Frisch et al., Gaussian, Inc., Wallingford CT, **2004**. For full reference see Supporting Information.
[33] R. Ahlrichs, M. Baer, M. Haeser, H. Horn, C. Koelmel, *Chem. Phys. Lett.* **1989**, *162*, 165.
[34] a) A. D. Becke, *Phys. Rev. A* **1988**, *38*, 3098; b) J. P. Perdew, *Phys. Rev. B* **1986**, *33*, 8822.
[35] A. Schaefer, H. Horn, R. Ahlrichs, *J. Chem. Phys.* **1992**, *97*, 2571.
[36] P. Deglmann, F. Furche, R. Ahlrichs, *Chem. Phys. Lett.* **2002**, *362*, 511.
[37] a) C. Møller, M. S. Plesset, *Phys. Rev.* **1934**, *46*, 618; b) J. S. Binkley, J. A. Pople *Int. J. Quantum Chem.* **1975**, *9S*, 229.
[38] F. Weigend, R. Ahlrichs, *Phys. Chem. Chem. Phys.* **2005**, *7*, 3297.
[39] a) K. Eichkorn, O. Treutler, H. Ohm, M. Häser, R. Ahlrichs, *Chem. Phys. Lett.* **1995**, *242*, 652; b) F. Weigend, *Phys. Chem. Chem. Phys.* **2006**, *8*, 1057.
[40] S. Grimme, *J. Chem. Phys.* **2003**, *118*, 9095.
[41] A. E. Reed, L. A. Curtiss, F. Weinhold, *Chem. Rev.* **1988**, *88*, 899.
[42] R. F. W. Bader, *Atoms in Molecules: A Quantum Theory*, Oxford University Press, Oxford, **1990**.
[43] a) AIMPAC, http://www.chemistry.mcmaster.ca/aimpac; b) A. Krapp, unpublished results.
[44] H.-J. Werner, P. J. Knowles, R. Lindh, F. R. Manby, M. Schütz, MOLPRO, version 2006.1, a package of ab initio programs; see http://www.molpro.net.
[45] a) F. M. Bickelhaupt, E. J. Baerends in *Reviews In Computational Chemistry, Vol. 15*, Wiley, New York, **2000**, p. 1; b) G. Te Velde, F. M. Bickelhaupt, E. J. Baerends, C. Fonseca Guerra, S. D. J. A. Van Gisbergen, J. Snijders, T. Ziegler, *J. Comput. Chem.* **2001**, *22*, 931.
[46] J. G. Snijders, E. J. Baerends, P. Vernoojs, *At. Data Nucl. Data Tables* **1982**, *26*, 483.
[47] J. Krijn, E. J. Baerends, Fit Functions in the HFS-Method, Internal Report (in Dutch), Vrije Universiteit Amsterdam, The Netherlands, **1984**.
[48] a) E. Van Lenthe, E. J. Baerends, J. G. Snijders, *J. Chem. Phys.* **1993**, *99*, 4597; b) E. Van Lenthe, E. J. Baerends, J. G. Snijders, *J. Chem. Phys.* **1994**, *101*, 9783; c) E. Van Lenthe, A. Ehlers, E. J. Baerends, *J. Chem. Phys.* **1999**, *110*, 8943.
[49] K. Morokuma, *J. Chem. Phys.* **1971**, *55*, 1236.
[50] a) T. Ziegler, A. Rauk, *Inorg. Chem.* **1979**, *18*, 1755; b) T. Ziegler, A. Rauk, *Inorg. Chem.* **1979**, *18*, 1558.
[51] F. M. Bickelhaupt, N. M. M. Nibbering, E. M. Van Wezenbeek, E. J. Baerends, *J. Phys. Chem.* **1992**, *96*, 4864.
[52] a) G. Frenking, K. Wichmann, N. Fröhlich, C. Loschen, M. Lein, J. Frunzke, V. M. Rayón, *Coord. Chem. Rev.* **2003**, *238–239*, 55; b) M. Lein, G. Frenking in *Theory and Applications of Computational Chemistry: The First 40 Years* (Eds.: C. E. Dykstra, G. Frenking,

K. S. Kim, G. E. Scuseria), Elsevier, Amsterdam, **2005**, p. 367; c) A. Krapp, F. M. Bickelhaupt, G. Frenking, *Chem. Eur. J.* **2006**, *12*, 9196.
[53] V. Jonas, G. Frenking, M. T. Reetz, *J. Am. Chem. Soc.* **1994**, *116*, 8741.
[54] E. A. V. Ebsworth, T. E. Fraser, D. W. H. Rankin, O. Gasser, H. Schmidbaur, *Chem. Ber.* **1977**, *110*, 3508.
[55] E. A. V. Ebsworth, T. E. Fraser, D. W. H. Rankin, *Chem. Ber.* **1977**, *110*, 3494.
[56] N. W. Mitzel, D. H. Brown, S. Parsons, P. T. Brain, C. R. Pulham, D. W. H. Rankin, *Angew. Chem.* **1998**, *110*, 1767; *Angew. Chem. Int. Ed.* **1998**, *37*, 1670.
[57] The geometry of **4** was previously calculated at the BP86/TZP level: R. Bertani, M. Casarin, P. Ganis, C. Maccato, L. Pandolfo, A. Venzo, A. Vittadini, L. Zanotto, *Organometallics* **2000**, *19*, 1373.
[58] Following IUPAC rules the name for $C(PPh_3)$ should be 1,3-bis(triphenyl)-1λ^5,3λ^5-diphosphapropadiene. The old name "phosphorane" for a P^V species is retained in the trivial name for the sake of simplicity.
[59] M. Tanimoto, K. Kuchitsu, Y. Morino, *Bull. Chem. Soc. Jpn.* **1970**, *43*, 2776.
[60] A. Ellern, T. Drews, K. Seppelt, *Z. Anorg. Allg. Chem.* **2001**, *627*, 73.
[61] a) H. G. Viehe, Z. Janousek, R. Gompper, D. Lach, *Angew. Chem.* **1973**, *85*, 581; *Angew. Chem. Int. Ed. Engl.* **1973**, *12*, 566; b) E. Oeser, *Chem. Ber.* **1974**, *107*, 627; c) R. Gompper, J. Schelble, C. S. Schneider, *Tetrahedron Lett.* **1978**, *19*, 3897; d) M. J. Taylor, P. W. J. Surman, G. R. Clark, *J. Chem. Soc. Chem. Commun.* **1994**, 2517.
[62] S. Grimme, *J. Phys. Chem. A* **2005**, *109*, 3067.
[63] Calculated from the experimental values for the heats of formation ΔH_f^{298} of C_3O_2 ($-22.4\,kcal\,mol^{-1}$), CO ($-26.4\,kcal\,mol^{-1}$) and $C(^3P)$ ($171.3\,kcal\,mol^{-1}$) taken from NIST Webbook http://webbook.nist.gov.
[64] K. P. Huber, G. Herzberg, *Molecular Spectra and Molecular Structure IV. Constants of Diatomic Molecules*, Van Nostrand-Reinhold, New York, **1979**.
[65] A. Beste, O. Krämer, A. Gerhard, G. Frenking, *Eur. J. Inorg. Chem.* **1999**, 2037.
[66] S. Erhardt, G. Frenking, *Chem. Eur. J.* **2006**, *12*, 4620.
[67] This does not mean that carbonyl complexes with little π backdonation from the acceptor moiety are weakly bonded. Complexes which have metal–CO σ bonds may be very strong. The have been termed non-classical carbonyls: A. J. Lupinetti, G. Frenking, S. H. Strauss, *Angew. Chem.* **1998**, *110*, 2229; *Angew. Chem. Int. Ed.* **1998**, *37*, 2113. For a review of non-classical carbonyls, see ref. [20b].

Received: September 4, 2007
Revised: December 10, 2007
Published online: March 3, 2008

